Available online at www.sciencedirect.com
ScienceDirect
Procedia Engineering 99 (2015) 1228 – 1233
Procedia Engineering
www.elsevier.com/locate/procedia

"APISAT2014", 2014 Asia-Pacific International Symposium on Aerospace Technology, APISAT2014

Topology Optimization Method Research on Hollow Wide-Chord Fan Blade of a High-bypass Turbofan Engine

J. MENG*, L.F. Liao, D. Li, Y. Cao, L.Y. Yang, Y.Y. Chen

ACAE, No. 3998 Lianhua Road, Shanghai 201108, China

Abstract

In order to realize lightweight design of a high-bypass turbofan engine, topology optimization of vacuum structure on a wide-chord fan blade was carried out regarding mixed loading conditions as static strength, vibration and bird-strike. Without changing the leaf shape, relationship of performance indices on vacuum structure was analyzed with simplified mechanical model of loading conditions. Topology optimization designs were carried out according to the highly sensitive conditions. Vacuum structure layout of fan blade was constructed integrating the major load transfer paths in each design proposal. Performance indices of different fan blade structures were compared. Result shown that optimized fan blade can realize lightweight as well as meeting the strength design requirement.

Peer-review under responsibility of Chinese Society of Aeronautics and Astronautics (CSAA)

Keywords: Topology optimization; Hollow fan blade; Mixed load conditions; Simplified mechanical model; Fork-shaped reinforcement ribs

1. Introduction

With the progress of modern turbine engine, dimension of fan blade continued increasing that brought great challenge to engine design both in strength requirement and weight control [1,2]. Typical structure of hollow Titanium alloy fan blade was shown in Fig. 1. With top and bottom sheet constituting the outside leaf shape, corrugated reinforcement ribs supported the fan blade. During high speed rotating, fan blade needed to meet stiffness and strength requirement under aerodynamic and centrifugal force. With the reinforcement structure

* Corresponding author. Tel.: +86-021-33367249; fax: +86-021-33366688.
E-mail address: mj_acae@126.com

1877-7058
Peer-review under responsibility of Chinese Society of Aeronautics and Astronautics (CSAA)
doi:10.1016/j.proeng.2014.12.652

distributed in radial direction, bending stiffness around Z-direction but not X-direction was improved. Without loading path from leading edge to root, strike force could not smoothly transmit in bird-strike. So the fan blade's stiffness and anti-bird-strike capability still needed to improve.

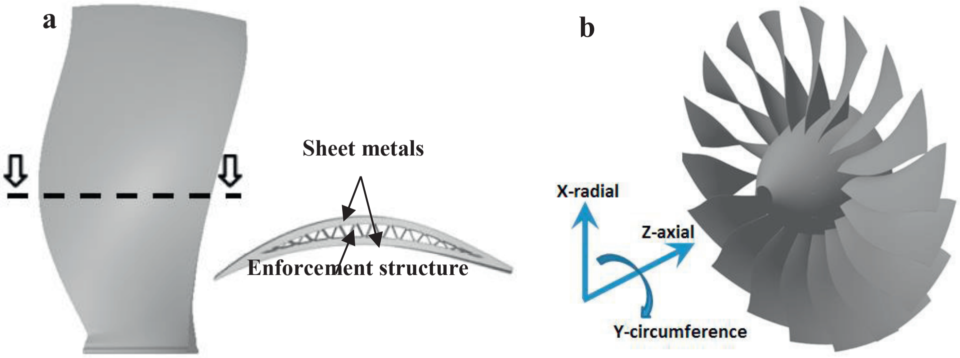

Fig. 1. Hollow fan blade. (a) blade structure; (b) working state.

As the leaf shape was decided by aerodynamic design, optimization is limited to internal reinforcement structure. Considering the complex structure along with mixed static, vibration and anti-bird-strike requirements, how to abstract and decompose this problem is key point of fan blade optimization [3,4].

In this research, topology optimization was carried out on decomposed mechanical models. Without changing the original leaf shape, reinforcement ribs of hollow fan blade was rearranged according to optimization result. Both lightweight and performance improvement were satisfied which provided a referable way for optimization of hollow fan blade.

2. Topology optimization of fan blade

2.1. Principal of topology optimization

Topology optimization's target is to find out the best material distribution to meet design requirement. Mathematical model of typical optimization problem is:

$$Minimize: f(x)=f(x_1, x_2, \dots x_i, \dots, x_n) \quad St: g_j(x) \leqslant 0 \ (j=1,2, \dots, m) \tag{1}$$

where are design variables, is optimization target and are design constraints. In topology optimization problems, density of each element was defined as design variables and varied between [0, 1]. Relationship between elastic modulus to density is:

$$E=E_0*\rho^d \tag{2}$$

where is original material's elastic module, E is the elastic module of optimized material, d is the dispersion coefficient. Combined with finite element (***FE***) method, each element's density was related to the properties of whole structure.

2.2. Estimation of original structure

Strength, vibration and bird-strike simulations of original fan blade were carried out to find out the dangerous position which could help to determine the design variables and constraints [5].

Static strength analysis was made by ANSYS and result was shown in Fig. 2(a). Max stress appeared at the transition zone between leading edge and blade root with value of 691MPa.

Mode analysis was also carried out by ANSYS and result was shown in Fig. 2(b). As shown in the Campbell Chart, the frequency margin between the second modal frequency (f2) and three times excitation was only 0.35% on working condition2 which may be dangerous of resonance.

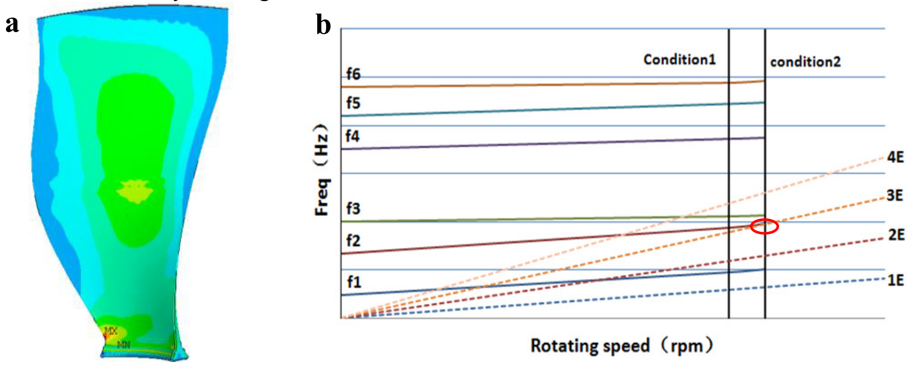

Fig. 2. Analysis result. (a) static strength analysis; (b) mode analysis.

Bird-strike analysis was carried out with fluid-structure coupling method by LS-DYNA [6-8]. As shown in Fig. 3(a), both rotation speed $\boldsymbol{V_1}$ and relative axial speed $\boldsymbol{V_2}$ were counted. Combination of velocities $\boldsymbol{V_{sum}}$ was applied on bird to strike the fixed fan blade. Analysis result was shown in Fig. 3(b). Material failure appeared at leading edge of the strike position and transition zone. Crack at transition zone may cause total blade body to fall off which could bring great challenge to containment of engine case and threaten the safety of occupants.

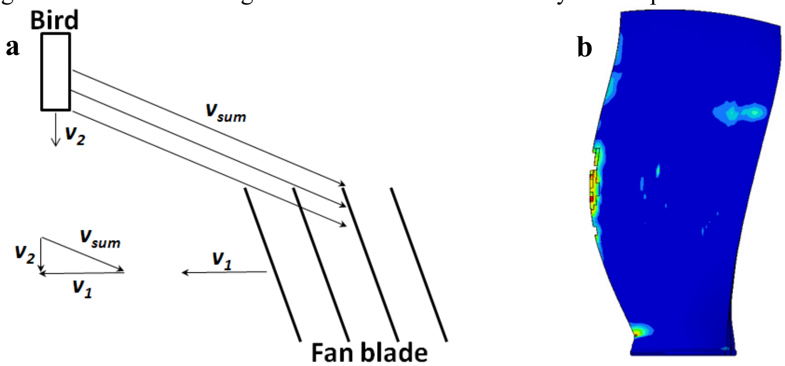

Fig. 3. Bird-strike analysis. (a) velocity combination method; (b) fan blade failure in bird-strike.

2.3. Decomposition of working subcases

2.3.1. Static strength subcase

It's concluded that most of static stress came from centrifugal force. As the least area section was the transition zone between blade and root, it was put out of the design region. For the blade, the centrifugal force was counted as:

$$F=mr\omega^2 \tag{3}$$

where $\boldsymbol{m}$ is the blade mass, $\boldsymbol{r}$ is the rotating diameter of the blade's center of gravity (***COG***) and $\boldsymbol{\omega}$ is the angular velocity. In order to maintain the static stress at transition zone, $\boldsymbol{r}$ shouldn't increase greatly after topology optimization.

2.3.2. Vibration subcase

As shown in Fig. 2(b), between major working ranges the frequency margin between excitation and natural frequency were too small to avoid resonance. One of the optimization targets was to increase the first three natural frequencies so as to raise the frequency margin.

2.3.3. Bird-strike subcase

Another one of the optimization target is to reduce the stress level at transition region to avoid fracture of whole blade. As shown in Fig. 3, the process of bird-strike could be decomposed to circumferential and axial strike. These two subcases would be included individually in optimization and stress at transition region would be constrained.

2.4. Design constraints and object

Without loss of generality, fan blade was simplified to a thick plate to get a more general optimization result. As shown in Fig. 4, the middle yellow region was defined as design region. By reference of the decomposed subcases, main constraint conditions of the plate were defined as followed：

- **Condition 1**: Constrained the bottom nodes and calculated modes of the plate. Result shown that the first modal frequency was 220.2Hz.
- **Condition 2**: Constrained the bottom nodes of plate and applied a static force of 1KN at 50% high of leading edge on X direction and –Z direction respectively. Results shown that max stresses at transition zone were 6.06MPa and 54.66MPa respectively.
- **Condition 3**: Constrained the bottom nodes of plate and applied a static force of 1KN at apex of leading edge on X direction and –Z direction respectively. Results shown that max stresses at transition zone were 11.14MPa and 89.80MPa respectively.

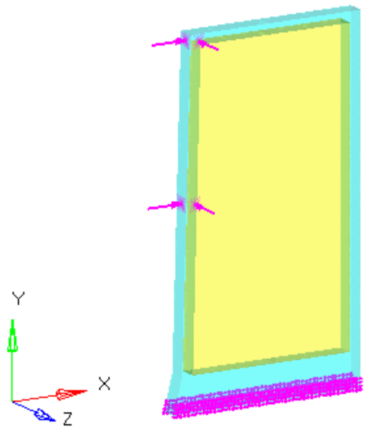

Fig. 4. Topology optimization strategy of simplified board

Design constraint: Consulting analysis result of three conditions with 50% vacuum anticipation, design constraint was defined as followed:

- In condition1, first modal frequency should be:

$$freq_1 \geqslant 150Hz \tag{4}$$

- In condition2, max stress at transition zone in two cases should be:

$$\sigma_x \leqslant 12MPa \qquad \sigma_{-z} \leqslant 110MPa \tag{5}$$

- In condition3, max stress at transition zone in two cases should be:

$$\sigma_x \leqslant 24MPa \qquad \sigma_{-z} \leqslant 180MPa \tag{6}$$

Design object: Minimize the mass of design region.

2.5. Optimization strategy

Iteration result and the optimization plate after rounding were shown in Fig. 5(a) and Fig. 5(b). In this model, fork-shaped reinforcement ribs contributed to the stiffness in all directions. Three ribs spread from upper left to bottom right that could help to transfer the strike force from leading edge to root. Verification of the Fork-shaped Hollow *(FH)* plate was shown in Table 1, this plate could meet design constraints with hollow ratio of 46.7%. According to the layout of optimization model, reinforcement ribs of original fan blade were rearranged and the *FH* fan blade was shown in Fig. 5(c).

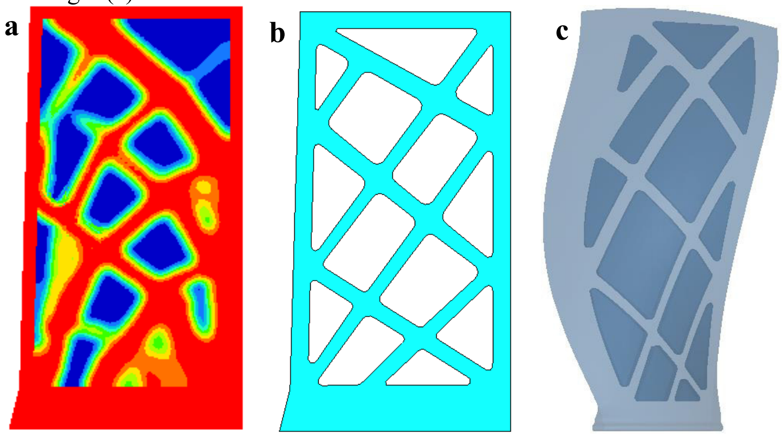

Fig. 5. Optimization result. (a) iteration result; (b) ***FH*** plate; (c) ***FH*** fan blade.

Table 1. Verification of ***FH*** plate.

	Design constraints	***Result***
Condition 1	$freq_1 \geqslant 150Hz$	*177.96Hz*
Condition 2	$\sigma_x \leqslant 12MPa$	*10.46MPa*
	$\sigma_{-z} \leqslant 110MPa$	103.51 MPa
Condition 3	$\sigma_x \leqslant 24MPa$	20.26 MPa
	$\sigma_{-z} \leqslant 180MPa$	172.83 MPa

3. Comparison between two fan blades

Verification analyses were carried out on ***FH*** fan blade and results were shown in Fig. 6. Comparisons with original fan blade were shown as followed:

- ***FH*** fan blade was 19.6% lighter than original fan blade.
- In static strength subcase, max stress reduced from 691MPa to 669MPa.
- In vibration subcase, the first three natural modal frequencies were efficiently increased. The lowest frequency margin was improved from 0.35% to 10.7% which effectively avoided resonance.
- In bird-strike subcase, no failure appeared at transition zone. Blade won't fall off from transition zone which would guarantee the safety of passengers.

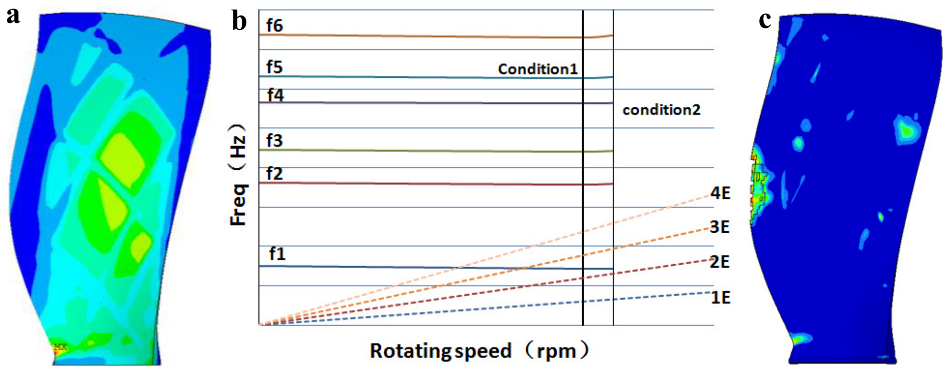

Fig. 6. Verification results of the ***FH*** fan blade. (a) static strength analysis; (b) mode analysis; (c) bird-strike analysis.

4. Summary and Prospect

In this research, optimization design was carried out on layout of inside reinforcement ribs of hollow fan blade. With the filling area between top and bottom sheets defined as the design region, topology optimization design was made regarding the combined mechanical properties and a new Fork-shaped Hollow fan blade was presented. By comparison with original fan blade, summaries were as followed:

1) The *FH* fan blade was 19.6% lighter than original fan blade;
2) For *FH* fan blade, performance in all the static strength, vibration and bird-strike was reduced while frequency margin and anti-strike capability had both improved

Unlike the corrugate shaped fan blade, *FH* fan blade could not be manufactured with SPF-DB technology. Additive Manufacturing (*AM*) technology was potential for the new fan blade. With the recently rapid progresses of *AM* in China, many factories and colleges were able to manufacture complicated Titanic structures which may provide an applicable method for the *FH* fan blade.

References

[1] P. Krammer, K. Rued,Truebenbach J., Technology preparation for green aero engines. AIAA–2003–22790.
[2] M.Z. Chen, B.J. Liu, Fan compressor aero design trend and challenge on the development of high bypass ratio turbofan, Journal of Aerospace Power. 23 (2008) 961–975.
[3] P.A. Parker, R. DeLoach, Structural optimization of a force balance using a computational experiment design. AIAA–2002–0540.
[4] J.Q. Yang, Y.R. Wang, Structural optimization of hollow fan blade based on orthogonal experimental design, Journal of Aerospace Power. 26 (2011) 376–384.
[5] A.I. Sayma, M. Vahdati, M. Imregun, An Integrated Nonlinear Approach for Turbomachinery Forced Response Prediction. Part I: Formulation, Journal of Fluids and Structures. 14 (2000) 87–101.
[6] S.H. Zhu, M.B. Tong, Y.Q. Wang, Experiment and numerical simulation of a fullscale aircraft windshield subjected to bird impact. AIAA–2009–2575.
[7] R. Jain, K. Ramachandra, Bird impact analysis of prestressed fan blades using explicit finite element code. Proceedings of the International Gas Turbine Congress, Tokyo, 2003.
[8] Y.N. Shmotin, P.V. Chupin, D.V. Gabov, Bird strike analysis of aircraft engine fan. 7th European LS-DYNA Conference, Salzburg, 2009.